DALTON
FULL PAPER

Synthesis, structure and magnetic properties of organic-intercalated bimetallic molecular-based ferrimagnets (n-C_nH_{2n+1})$PPh_3M^{II}Fe^{III}$-$(C_2O_4)_3$, (M^{II} = Mn, Fe; n = 3–7)

Ian D. Watts, Simon G. Carling and Peter Day *

Davy Faraday Research Laboratory, The Royal Institution of Great Britain, 21 Albemarle Street, London, UK W1S 4BS

Received 3rd August 2001, Accepted 25th January 2002
First published as an Advance Article on the web 7th March 2002

Bimetallic tris-oxalato-salts (n-C_nH_{2n+1})$PPh_3M^{II}Fe^{III}(C_2O_4)_3$ (n = 3–7, M^{II} = Mn, Fe) were prepared and the structures investigated by powder X-ray diffraction in order to study the evolution of the structure and magnetic properties as a function of alkyl chain length. The compounds all have the same two-dimensional honeycomb structure of M^{II} and Fe^{III} bridged by oxalate, with the organic cations lying between the metal–oxalate layers, whose separation ranges from 9.48 Å (n = 3) to 11.10 Å (n = 7) for the Fe^{II} salts and 9.37 to 10.81 Å for Mn^{II}. The compounds all behave as ferrimagnets, with magnetic parameters similar to the corresponding $AM^{II}Fe^{III}(C_2O_4)_3$ with A = NR_4^+, PPh_4^+ and T_cs almost insensitive to interlayer separation. The Mn^{II} salts exhibit uncompensated magnetisation below T_c and the Fe^{II} ones show Néel type N ferrimagnetism, with negative magnetisation at low temperature, the magnitude of which is influenced by the preparation conditions, due to vacancies in the Fe^{II} sublattice.

Introduction

Infinite lattices constructed by coordinating tris-oxalato-metallate(III) anions with divalent metal ions have provided numerous examples of unusual cooperative magnetic behaviour,[1] as well as novel lattice architectures.[2] The ambidentate $C_2O_4^{2-}$ transmits a relatively strong exchange interaction, which may be ferro- or antiferro-magnetic, according to the combination of M(II) and M(III).[3] Depending on size, shape and charge of organic cation A, compounds $AMM'(C_2O_4)_3$ can have two- or three-dimensional polymeric structures, with cations such as NR_4^+, PR_4^+ (R = n-alkyl or phenyl) consisting of honeycomb layers of alternating M and M′, with A occupying the space between the layers.[4,5] In view of the wide interest in low-dimensional spin systems, as exemplified for example by the layer perovskite halide salts,[6,7] it is pertinent to attempt to vary the distance between the layers by changing the length of the alkyl chains in the cations. Only a limited range of $(n\text{-}C_nH_{2n+1})_4NMM'(C_2O_4)_3$ can be prepared, with n = 3–5.[4] We have therefore synthesised $AMFe(C_2O_4)_3$ (M = Mn, Fe) salts containing a series of unsymmetrical cations (n-C_nH_{2n+1})PPh_3^+ with n = 3–7. The compounds behave as ferrimagnets, with magnetic parameters similar to the corresponding salts with symmetrical cations. In particular, the $Mn^{II}Fe^{III}$ salts show spin canting below T_c, while the $Fe^{II}Fe^{III}$ ones are Neél type N ferrimagnets with compensation temperatures and negative low temperature magnetisation.[4,8] Surprisingly, there is no clear correlation between the ordering temperatures and interlayer spacing in either series.

Experimental

Synthesis

All chemicals were purchased from Aldrich and used as supplied. Water was distilled in the laboratory.

$AMFe(C_2O_4)_3$ were synthesised by a modified version of the 'ionic' procedure.[9] 1.5 mmol of the cation in the form of the Cl or Br salt was dissolved in 5 ml methanol or water. The resulting solution was mixed with 5 ml of a 0.2 M solution of $Fe(NO_3)_3{\cdot}9H_2O$ in water. 1 mmol of solid $FeSO_4{\cdot}7H_2O$ or $MnCl_2{\cdot}4H_2O$, as appropriate, was added to the solution and agitated until dissolved. Typically six drops of 1 M HCl solution was added to suppress the formation of oxalate complexes of the divalent metal. Finally, 5 ml of a 0.6 M solution of oxalic acid was added, resulting in the formation of green ($Fe^{II}Fe^{III}$) or yellow ($Mn^{II}Fe^{III}$) microcrystals over a timescale from a few seconds to several hours. The product was collected and washed twice with 20 ml of water and twice with 20 ml of methanol, dried *in vacuo* over blue silica gel and stored in the dark.

In the (n-C_nH_{2n+1})$PPh_3MFe(C_2O_4)_3$ series, compounds containing the smaller cations (n = 3–5) form readily, the n = 5 derivates being the most crystalline, while for n = 6, 7 the products contained a substantial amorphous component. (n-$C_7H_{15}PPh_3$)$MnFe(C_2O_4)_3$ was the most difficult compound to synthesise since the cation tended to react with $MnCl_2{\cdot}4H_2O$. Hence, the divalent metal salt was added last to the reaction vessel in this case. Although synthesis of the n = 3–5 salts was relatively facile, varying the synthetic conditions had a marked influence on the magnetic behaviour of the products. These effects are described later.

Attempts to improve the crystallinity of compounds derived from symmetrical cations such as PPh_4^+ or $(n\text{-}C_4H_9)_4N^+$ by slow diffusion of the reactants in an H-cell or gel had been unsuccessful. Diffusion of the reactants through a glass frit yielded an improved sample of $(n\text{-}C_4H_9)_4NFe^{II}Fe^{III}(C_2O_4)_3$ but this technique was unsuccessful with the unsymmetrical alkyltriphenylphosphonium cations.

X-Ray diffraction

All compounds were initially characterised at room temperature using a Siemens D500 powder diffractometer in flat-plate geometry and monochromatic Cu-Kα_1 radiation. Additionally the diffraction profiles of the two most crystalline compounds, (n-C_5H_{11})$PPh_3M^{II}Fe^{III}(C_2O_4)_3$, were measured on the high-resolution diffractometer BM16 at the European Synchrotron Radiation Facility, Grenoble. The samples were mounted in sealed borosilicate glass capillaries of 0.7 mm diameter and

DOI: 10.1039/b107057f

Table 1 Elemental analysis of $(n\text{-}C_nH_{2n+1})PPh_3FeFe(C_2O_4)_3$ (calculated values in parentheses)

Compound	Percentage by weight			
	C	H	P	Fe
$n = 3$	48.37 (47.61)	3.13 (3.26)	4.67 (4.55)	15.57 (16.40)
$n = 4$	49.51 (48.38)	3.10 (3.48)	4.64 (4.46)	14.92 (16.07)
$n = 5$	50.25 (49.12)	3.68 (3.70)	4.53 (4.37)	14.52 (15.75)
$n = 6$	50.73 (49.82)	4.06 (3.90)	4.35 (4.28)	14.72 (15.44)
$n = 7$	51.77 (50.50)	4.28 (4.10)	4.40 (4.20)	14.28 (15.15)

Table 2 Elemental analysis of $(n\text{-}C_nH_{2n+1})PPh_3MnFe(C_2O_4)_3$ (calculated values in parentheses)

	Percentage by weight				
	C	H	P	Mn	Fe
$n = 3$	48.34 (47.68)	3.17 (3.26)	4.69 (4.55)	6.44 (8.08)	8.49 (8.21)
$n = 4$	49.53 (48.44)	3.57 (3.48)	4.70 (4.46)	6.51 (7.91)	7.82 (8.04)
$n = 5$	49.93 (49.18)	3.95 (3.70)	4.53 (4.37)	6.18 (7.76)	8.22 (7.88)
$n = 6$	50.30 (49.89)	4.00 (3.91)	4.52 (4.29)	6.67 (7.61)	7.99 (7.73)
$n = 7$	49.37 (50.57)	4.09 (4.11)	4.09 (4.21)	7.81 (7.46)	7.30 (7.58)

were rotated throughout the measurement. A wavelength of 0.800615 Å was chosen and calibrated with NBS (National Bureau of Standards) silicon.

Magnetometry

Temperature and magnetic field dependence of magnetisation was measured with a Quantum Design MPMS7 SQUID magnetometer. 10–20 mg of the sample was mounted in a gel cap which was held inside a plastic drinking straw. Three empty gel caps were inserted into the straw above and below the sample to provide a constant background in the range of the measurement coils. The straw was attached to the sample stick by adhesive Kapton tape. The measurement protocol was the same for all samples; the remnant field at the instrument setting of 0 Oe was determined at 100 K by applying small fields and measuring the SQUID response until a figure of $<10^{-6}$ emu was achieved. This field was then taken as zero. The sample was cooled in zero field and the magnetisation measured while warming in 100 Oe (allowing for the zero field correction) to 60 K. The sample was then cooled in the 100 Oe field and the magnetisation measured while warming to 300 K. The data were corrected for sample diamagnetism by use of Pascal's constants.[10]

Results

Elemental analysis

Found and calculated results of elemental analysis are presented in Tables 1 and 2. It is noticeable that all the $Fe^{II}Fe^{III}$ compounds are deficient in Fe, in common with other $AM^{II}M^{III}(C_2O_4)_3$ compounds which are deficient in the divalent metal.[4] Four of the $Mn^{II}Fe^{III}$ compounds also exhibit the same effect, except for the $n = 7$ one, for which the Mn^{II} content is higher than expected, probably due to a small contamination of the product of the reaction with $MnCl_2{\cdot}4H_2O$. Nevertheless, the structural and magnetic properties of $(n\text{-}C_7H_{15})PPh_3MnFe(C_2O_4)_3$ are similar to the other compounds

Crystal structures

Crystal structures have been determined for seven $AM^{II}M^{III}(C_2O_4)_3$ compounds from single crystal X-ray data, three of which are $Mn^{II}Fe^{III}$ compounds.[5,11,12] In contrast, no structures based on single crystal X-ray data have been published for any $AFe^{II}Fe^{III}(C_2O_4)_3$ compounds. However, powder X-ray diffraction indicates that all the $AM^{II}M^{III}(C_2O_4)_3$ compounds have similar layered structures. In general, compounds containing the unsymmetrical cations $(n\text{-}C_nH_{2n+1})PPh_3$ are less crystalline than those formed from symmetrical cations such as $(n\text{-}C_4H_9)_4N$ and PPh_4. As a result, determination of lattice parameters by the usual method of finding the peak positions and refining the unit cell was not possible. Consequently, the *c* axes were determined from the 0 0 l reflections, and the *a* and *b* axes by carrying out LeBail extractions using the program GSAS,[13] by fixing *c* and allowing *a* and *b* to vary.

Layered bimetallic tris-oxalato-salts suffer from stacking faults, resulting in contributions to the diffraction pattern from two phases, *R*3*c* and $P6_3$. LeBail extractions using both space groups together failed. Thus the space group $P6_5$, which includes all the reflections from *R*3*c* and $P6_3$, was used for the extraction in all except C_7 compounds for which the best fit was achieved in the orthorhombic space group $C222_1$. Other $AM^{II}M^{III}(C_2O_4)_3$ compounds have been found to crystallise in this space group, notably $(n\text{-}C_5H_{11})_4NFeFe(C_2O_4)_3$[4] and $(n\text{-}C_5H_{11})_4NMnFe(C_2O_4)_3$.[5] The effect of crystallisation in $C222_1$ is that the tris-oxalato-metallate site symmetry is lowered from C_3 (for $P6_3$) to C_2. The vastly greater resolution of the BM16 diffractometer as compared to the laboratory instrument allows us to further resolve the profiles of the two C_5 compounds. Whilst structures have not yet been determined for these materials, it is readily apparent that the symmetry is much lower than hexagonal. Good matches to the observed profiles have been achieved using the LeBail method, with a monoclinic cell in space group $P2_1$; the fit for $(n\text{-}C_5H_{11})PPh_3MnFe(C_2O_4)_3$ is shown in Fig. 1. The unit cell parameters derived from the higher resolution data are $a = 9.4353(2)$ Å, $b = 19.7599(3)$ Å, $c = 9.5432(3)$ Å, $\beta = 121.035(2)°$ for $(n\text{-}C_5H_{11})PPh_3MnFe(C_2O_4)_3$ and $a = 9.4251(8)$ Å, $b = 19.822(1)$ Å, $c = 9.551(1)$ Å, $\beta = 121.154(4)°$ for $(n\text{-}C_5H_{11})PPh_3FeFe(C_2O_4)_3$. The weighted profile *R*-factors of the two fits are 6.5% and 10.2% respectively. In these cases the stacking axis is now *b* and the layer is somewhat distorted from hexagonal geometry.

These unit cell parameters can be compared with those determined from laboratory data for all the compounds, which are presented in Table 3. The parameters for $(n\text{-}C_4H_9)_4NMnFe(C_2O_4)_3$, $PPh_4MnFe(C_2O_4)_3$ and $PPh_4FeFe(C_2O_4)_3$,[8] and for $(n\text{-}C_4H_9)_4NFeFe(C_2O_4)_3$, grown by slow diffusion, are also included. It has been reported[14] that cation disorder in the $AM^{II}M^{III}(C_2O_4)_3$ series results in a doubling of the *a* and *b* axes, particularly for compounds containing PPh_4^+, and a similar effect is found in the compounds containing alkyltriphenylphosphonium cations.

The 0 0 l peaks shift to lower 2θ with increasing *n* of the

Table 3 Lattice parameters for $AMFe(C_2O_4)_3$ compounds

		Space group	*a*/Å	*b*/Å	*c*/Å
Fe^{II}, Fe^{III}	$n = 3$	*P*6(5)	18.64(5)		56.92(3)
	$n = 4$	*P*6(5)	18.62(3)		57.76(2)
	$n = 5$	*P*6(5)	18.49(9)		60.9(5)
	$n = 6$	*P*6(5)	18.81(5)		62.9(5)
	$n = 7$	$C222_1$	16.82(3)	31.32(2)	22.1(1)
	$(n\text{-}C_4H_9)_4N^+$	*R*3*c*	9.39(1)		53.75(5)
	PPh_4^{+8}	*P*6(5)	18.76(2)		57.1(1)
Mn^{II}, Fe^{III}	$n = 3$	*P*6(5)	18.96(2)		56.22(5)
	$n = 4$	*P*6(5)	18.81(1)		57.24(5)
	$n = 5$	*P*6(5)	18.76(1)		59.3(3)
	$n = 6$	*P*6(5)	18.90(3)		60.8(2)
	$n = 7$	$C222_1$	16.1(5)	30.4(8)	21.63(2)
	$(n\text{-}C_4H_9)_4N^{+8}$	*R*3*c*	9.47(1)		53.5(1)
	PPh_4^{+8}	*P*6(5)	18.87(2)		56.84(5)

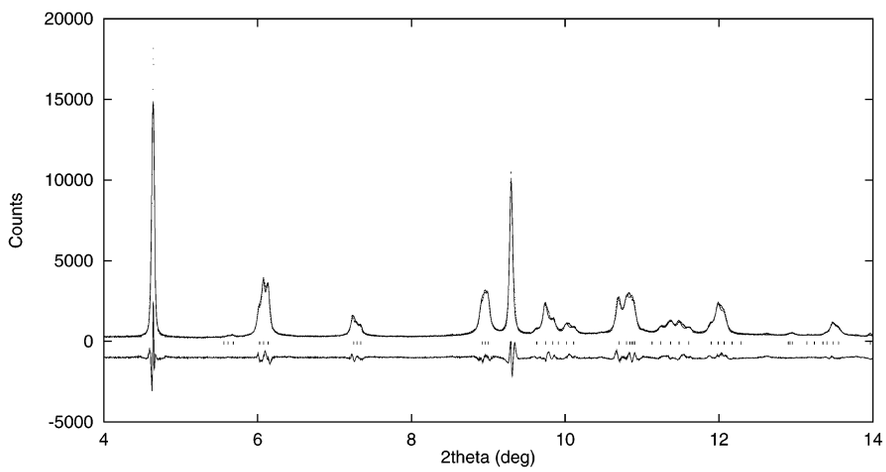

Fig. 1 LeBail extraction of the X-ray powder diffraction profile of $(n\text{-}C_5H_{11})PPh_3MnFe(C_2O_4)_3$.

cation, corresponding to an increase in the *c* axis and interlayer separation. Comparison of the increase in interlayer separation for the two series highlights a similar dependence on the alkyl chain length of the cation (Fig. 2). In both series, increasing

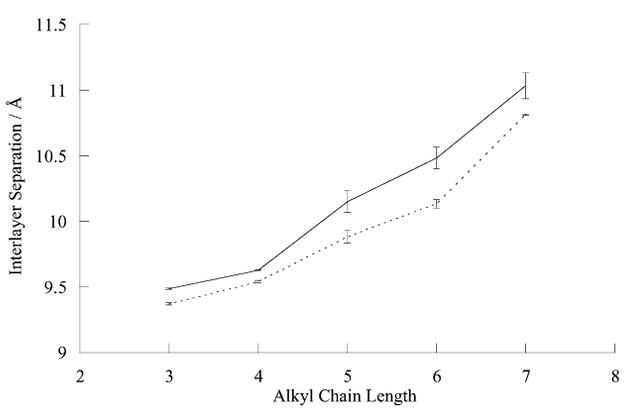

Fig. 2 Interlayer spacing *vs.* *n* for $(n\text{-}C_nH_{2n+1})PPh_3MFe(C_2O_4)_3$ (M = Mn, dotted line; M = Fe, solid line).

alkyl chain length gives rise to the well-known alternation effect whereby increasing the number of carbons from even to odd increases the interlayer separation more than from odd to even. Fig. 2 also reveals that the interlayer separation in the MnFe series is consistently smaller than in the FeFe series, due to the difference in the ionic radii of Mn^{II} and Fe^{II}. As that of Mn^{II} is larger than Fe^{II}, the honeycomb 'pore' size in the MnFe series is slightly larger than the FeFe series. Consequently the cation is able to penetrate further into the tris-oxalato-metallate layer, decreasing the interlayer separation.

Magnetic properties

$Mn^{II}Fe^{III}$ compounds. Fig. 3 shows the temperature-dependent magnetisations of the $(n\text{-}C_nH_{2n+1})PPh_3MnFe(C_2O_4)_3$ (n = 3–7) compounds recorded on warming after cooling in a 100 Oe field. They all feature a broad maximum at ≈50 K and a rapid increase in magnetisation at lower temperature. Similar behaviour has been found in other $AMnFe(C_2O_4)_3$ compounds,[4] the broad maxima (Fig. 3(a)) being characteristic of Heisenberg two-dimensional antiferromagnetism.[6] The quantity $\chi_{max}T(\chi_{max})/C$, where χ_{max} = the susceptibility of the maximum, $T(\chi_{max})$ = the temperature of the maximum and C = Curie constant, has been calculated for ideal two-dimensional antiferromagnets for various lattice topologies and spin values from high-temperature series expansions.[6,15] For a honeycomb lattice of S = 5/2 spins it is 0.330, assuming an isotropic Landé g factor of 2. The values found range from 0.23–0.28, suggesting some deviation from ideal two-dimensional behaviour.

The sharp increase in magnetisation at lower temperature indicates a remaining uncompensated moment in the antiferromagnetic state. This has recently been reported to be due to spin-canting by Mössbauer studies on $(n\text{-}C_5H_{11})_4NMnFe(C_2O_4)_3$.[16] An alternative explanation, however, is that the deficiency of manganese found in most of these compounds is responsible for the uncompensated magnetisation. The fact that the spontaneous magnetisation is parallel to the crystallographic *c*-axis,[5] which has also been found to be the orientation of the antiferromagnetic spins in the ordered phase,[17] tends to support the latter hypothesis. It should be noted that the form of the increase in magnetisation for $(n\text{-}C_7H_{15})PPh_3MnFe(C_2O_4)_3$ is different from the other members of the series, presumably as a consequence of the excess Mn found in the

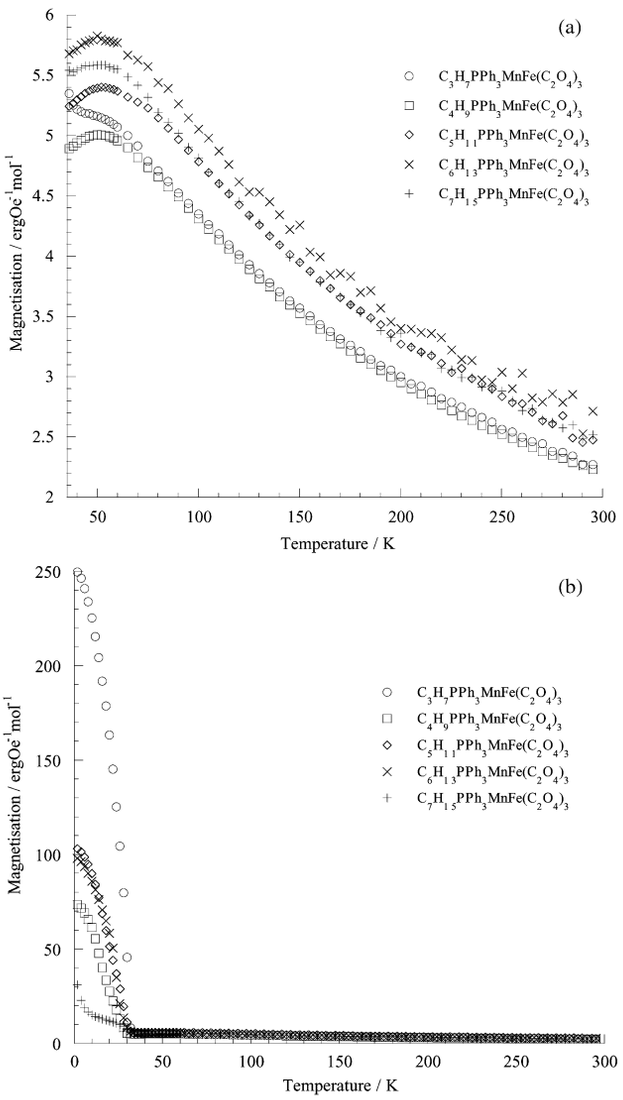

Fig. 3 Temperature-dependent field-cooled magnetisation of (n-C_nH_{2n+1})$PPh_3MnFe(C_2O_4)_3$, (a) from 300–352 K; (b) from 2–300 K.

elemental analysis. However, the major contribution arises from the honeycomb metal-trisoxalate layers, as borne out by the similarity of the maxima in Fig. 3(a) which suggests that the deviation in behaviour at low temperature is due to a small paramagnetic impurity.

The transition to full long-range magnetic order was determined as the temperature at which the field-cooled magnetisation diverged from the zero-field-cooled curve as shown in Fig. 4. Curie and Weiss constants were obtained from fits of

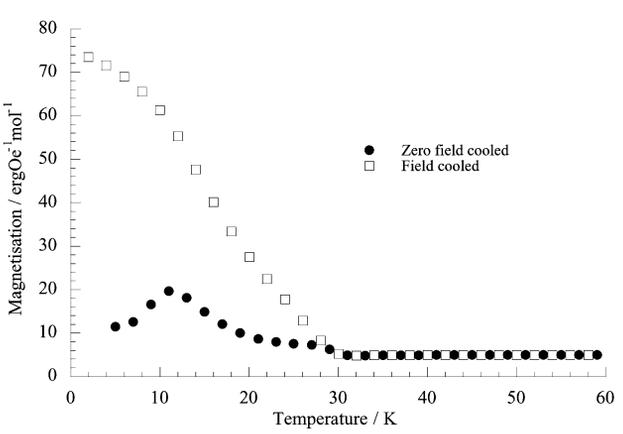

Fig. 4 Temperature-dependent field-cooled and zero-field-cooled magnetisation of (n-$C_4H_9PPh_3$)$MnFe(C_2O_4)_3$.

inverse susceptibility against temperature in the paramagnetic region. Magnetic parameters are summarised in Table 4, values for the $(n\text{-}C_4H_9)_4N^+$ and PPh_4^+ salts are also included for comparison.[4] The large negative Weiss constants confirm the strongly antiferromagnetic nature of the magnetic exchange.

$Fe^{II}Fe^{III}$ compounds. Fig. 5 shows the temperature-dependent

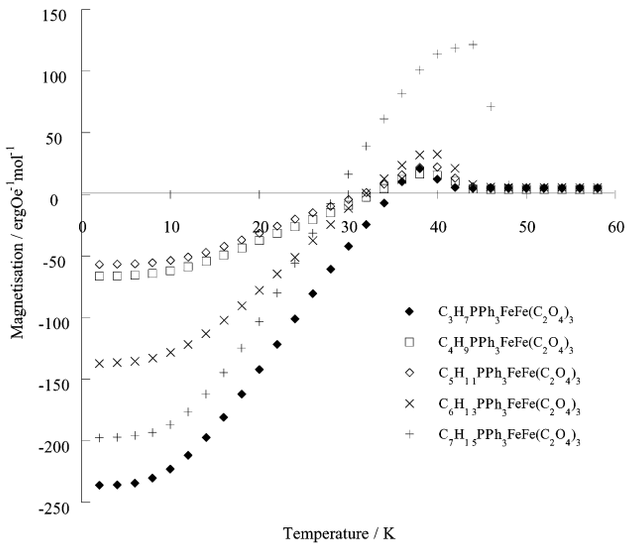

Fig. 5 Temperature-dependent field-cooled magnetisation of (n-C_nH_{2n+1})$PPh_3FeFe(C_2O_4)_3$.

magnetisation of the $Fe^{II}Fe^{III}$ compounds, recorded on warming after cooling in a 100 Oe magnetic field. Again, the behaviour of all the compounds is similar in that the magnetisation below the ordering temperature is initially positive but, after reaching a maximum, decreases with decreasing temperature through a compensation point where there is zero net magnetisation, to negative magnetisation at low temperature. This type of behaviour, corresponding to Néel type N ferrimagnetism was first observed in $AFe^{II}Fe^{III}(C_2O_4)_3$ compounds by Mathonière *et al.*[4] Magnetic parameters are summarised in Table 5 with values for the $(n\text{-}C_4H_9)_4N^+$ and PPh_4^+ salts included for comparison.[8] The large negative Weiss constants indicate again that the magnetic exchange is strongly antiferromagnetic. Table 5 reveals that the magnetic parameters vary between compounds somewhat more than for the MnFe compounds. As in the MnFe series, this variation is most likely due to small differences in the divalent/trivalent metal ratio, although varying crystallinity among the compounds and the contributions from the $R3c$ and $P6_3$ phases could also contribute.

Negative magnetisation has also been reported for other $AFe^{II}Fe^{III}(C_2O_4)_3$ compounds,[4] and the only compounds of this type that do not display this property are those containing PPh_4^+ and $AsPh_4^+$.[8,18] Especially noteworthy in the present case is the occurrence of either negative or positive low temperature magnetisation, depending on the precise details of the preparation procedure. An example is shown in Fig. 6. The two samples displaying positive magnetisation at low temperature were synthesised by mixing ethanolic solutions of the cation with aqueous solutions of $Fe(NO_3)_3{\cdot}9H_2O$, $FeSO_4{\cdot}7H_2O$ and oxalic acid, with addition of 6 drops of 1 M HCl. The sample displaying negative magnetisation was synthesised in the same way, except that the cation was dissolved in methanol. Positive low temperature magnetisation was also found for samples which had been synthesised from methanolic solutions of all the components, synthesised under cooler or more acidic conditions or precipitated from excess solvent. More detailed study of the synthesis conditions was therefore made, using the C_3 salt as an example. X-Ray powder diffraction profiles showed that

Table 4 Magnetic parameters for $AMnFe(C_2O_4)_3$

A	T_c/K	C/erg Oe^{-2} mol^{-1} K	θ/K	μ_{eff}/μ_B (2 K)
$(n\text{-}C_3H_7)PPh_3^+$	32.5(2)	9.03(7)	−101(2)	0.0447
$(n\text{-}C_4H_9)PPh_3^+$	30.0(2)	8.8(2)	−97.4(6)	0.0132
$(n\text{-}C_5H_{11})PPh_3^+$	33.2(2)	10.1(2)	−83(7)	0.0185
$(n\text{-}C_6H_{13})PPh_3^+$	33.0(2)	11.7(4)	−113(12)	0.0175
$(n\text{-}C_7H_{15})PPh_3^+$	32.9(2)	10.7(1)	−99(4)	0.0022
$(n\text{-}C_4H_9)_4N^+$ [4]	26.0(2)	10.5(5)	−101(4)	0.0065
PPh_4^+ [4]	23.5(2)	7.3(3)	−111(12)	0.0033

Table 5 Magnetic parameters for $AFeFe(C_2O_4)_3$

A	T_c/K	C/erg Oe^{-2} mol^{-1} K	θ/K
$(n\text{-}C_3H_7)PPh_3^+$	42(1)	8.79(4)	−87(2)
$(n\text{-}C_4H_9)PPh_3^+$	44(1)	7.3(1)	−85(4)
$(n\text{-}C_5H_{11})PPh_3^+$	44(1)	8.9(1)	−88(4)
$(n\text{-}C_6H_{13})PPh_3^+$	44(1)	9.6(1)	−101(4)
$(n\text{-}C_7H_{15})PPh_3^+$	48(1)	8.83(2)	−88.0(7)
$(n\text{-}C_4H_9)_4N^+$ [8]	45	7.88(1)	−90.2(3)
PPh_4^+ [8]	34	6.7(1)	−88.4(2)

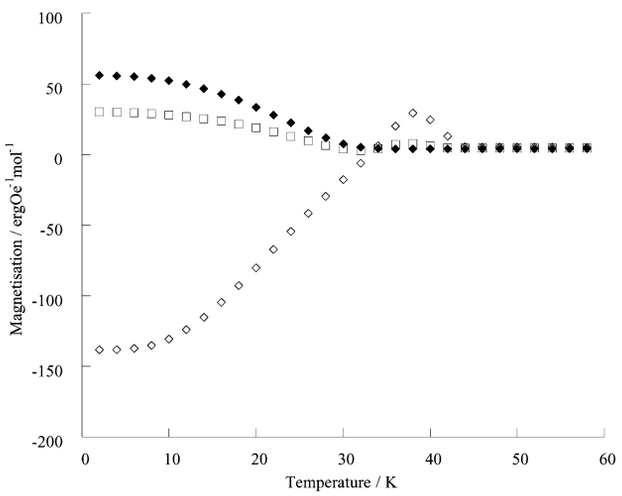

Fig. 6 Temperature-dependent field-cooled magnetisation of three samples of $(n\text{-}C_4H_9)PPh_3FeFe(C_2O_4)_3$.

the magnetic variations were not due to major structural changes but elemental analysis revealed a correlation between the magnetic behaviour and the Fe deficiency. The sample with the greatest negative magnetisation has the smallest Fe deficiency while the sample with positive magnetisation has the greatest deficiency.

Discussion

Powder X-ray diffraction profiles show that compounds containing alkyltriphenylphosphonium cations are much less crystalline than those of symmetrical cations such as PPh_4^+ or $(n\text{-}C_4H_9)_4N^+$. In addition, they are more prone to stacking faults between the layers. Nevertheless, lattice parameters have been determined by means of LeBail extractions and the space groups used for the extractions are similar to other compounds of this type. Structures determined from single crystal diffraction data have been assigned to the orthorhombic $C222_1$ or hexagonal $R3c$ space groups. Lattice parameters are comparable to other compounds of the $AMM'(C_2O_4)_3$ type. The a axis varies between 18.49 Å and 18.96 Å while the c axis ranges from 56.22 Å for $(n\text{-}C_3H_7PPh_3)MnFe(C_2O_4)_3$ to 66.20 Å for $(n\text{-}C_7H_{15})PPh_3FeFe(C_2O_4)_3$ (converting from the $C222_1$ space group for the latter compound for ease of comparison). By comparison, the smallest and largest c axes reported are 49.207 Å and 87.1 Å for $(n\text{-}C_3H_9)_4NMnCr(C_2O_4)_3$ [16] and $[N(PPh_3)_2]MnFe(C_2O_4)_3$ [4] respectively. As the alkyltriphenylphosphonium series fall in the middle of this range, it would be interesting to determine the upper limit for the length of the alkyl chain. Preparations derived from $(n\text{-}C_nH_{2n+1})PPh_3^+$ where $n \geq 8$ could not be carried out due to non-availability of the cations, while syntheses of $(n\text{-}C_{12}H_{25})PPh_3^+$ salts were unsuccessful. Bimetallic tris-oxalato-salts containing tetra-*n*-alkylammonium cations are restricted to $(C_nH_{2n+1})_4N^+$ (n = 3–5), suggesting that the limiting factor is not the interlayer separation, but the size of the cation that can be accommodated before it interferes with its neighbour. In view of the difficulty in synthesising the $(n\text{-}C_6H_{13})PPh_3^+$ and $(n\text{-}C_7H_{15})PPh_3^+$ derivatives, the upper limit in alkyl chain length may already have been reached in this series.

The increase in interlayer separation with increasing n demonstrates the alternation effect in a similar fashion for both MnFe and FeFe series, and the magnitude of the increase supplies evidence for the orientation of the unsymmetrical cations. Turning to related compounds, single crystal diffraction data on $PPh_4MnCr(C_2O_4)_3$ [12] and $(n\text{-}C_5H_{11})_4NMnFe(C_2O_4)_3$ [5] reveals two different modes of cation orientation. In the PPh_4^+ case, one of the phenyl rings penetrates the honeycomb layer, while the others occupy the space between the layers. In contrast, two of the alkyl chains of $(n\text{-}C_5H_{11})_4N^+$ lie in the *ab* plane while the other two are in a plane perpendicular to it, so that only the terminal methyl groups of two of the chains penetrate the layers, one above and one below the cation. The a axis in $PPh_4MnCr(C_2O_4)_3$ is doubled because the honeycomb layer is distorted away from ideal hexagonal symmetry. Thus three of the hexagons in the unit cell are elongated by the orientations of the penetrating phenyl rings while the fourth is occupied by a disordered ligand and is not distorted.

Doubling of the a axis is also necessary in fitting the powder diffraction profiles of the unsymmetrical alkyltriphenylphosphonium salts, which suggests that one of the phenyl rings also penetrates the layer in these compounds. The simplest hypothesis is that the cation adopts the same orientation in each compound, keeping the alkyl chain at the same angle, when the increase in interlayer separation would equate to extending the chain by one carbon. Fixing the mean angle of the alkyl chain gives a prediction for the increase in interlayer separation on adding one carbon.

However, under these circumstances, the predicted increase in interlayer separation on extending the alkyl chain from C_4 to C_5 is 1.49 Å, whereas the observed increase is only 0.52 Å. This suggests that the conformation adopted is such that the terminal C–C bond is twisted away from the c axis, to instead make a small angle with the a axis and thus limit the increase in interlayer separation. Another possibility is that the alkyl chains are not all *trans*-configuration but contain one, or more, *gauche* bonds, as with the terminal bond of the pentyl chains of $(n\text{-}C_5H_{11})_4NMnFe(C_2O_4)_3$.[5] Changes in the a axis suggest that the cation's penetration of the layer decreases from C_3 to C_5, increases to C_6 and reduces again for C_7. This variation does not correlate with that of the interlayer separation, but it is noteworthy that it is similar in both MnFe and FeFe compounds.

For certain alkyltriphenylphosphonium cations, modifying the synthetic conditions had a marked influence on the magnetic behaviour of the resultant compounds. Variation of solvent, pH, temperature, amount of solvent and concentration

of the cation solution all affect the magnitude of the low-temperature magnetisation. The widest variation, both positive and negative at low temperature, was found to arise from different molarities of the cation solution in preparations of $(n\text{-}C_3H_7PPh_3)FeFe(C_2O_4)_3$. Chemical analysis indicates that it results from deficiency of Fe^{II}. Increasing deficiency results in a decrease in the magnitude of the negative low temperature magnetisation, the most deficient samples actually showing positive magnetisation, and no compensation temperature.

The general conclusion is that a substantial variation of the alkyl chain length in $(n\text{-}C_nH_{2n+1})PPh_3MFe(C_2O_4)_3$, M = Mn and Fe, from 3 to 7 causes only a modest expansion of the interlayer spacing, and has no significant effect on the magnetic parameters. Most probably, this is because the alkyl chains lie nearly parallel to rather than perpendicular to the magnetic layers.

Acknowledgements

This work was supported by the EPSRC. The authors wish to thank the ESRF for access to beamtime and Dr Olivier Masson for assistance with measurements.

References

1 C. Mathonière, S. G. Carling, Dou Yusheng and P. Day, *J. Chem. Soc., Chem. Commun.*, 1994, 1551.
2 S. Decurtins, H. W. Schmalle and H. R. Oswald, *Inorg. Chem.*, 1993, **32**, 1888.
3 H. Tamaki, Z. Zhong, N. Matsumoto, S. Kida, M. Koikawa, N. Aihiwa, Y. Hashimoto and H. Okawa, *J. Am. Chem. Soc.*, 1992, **114**, 6974.
4 C. Mathonière, C. J. Nuttall, S. G. Carling and P. Day, *Inorg. Chem.*, 1996, **35**, 1201.
5 S. G. Carling, C. Mathonière, P. Day, K. M. A. Malik, S. J. Coles and M. B. Hursthouse, *J. Chem. Soc., Dalton Trans.*, 1996, 1839.
6 L. J. de Jongh and A. R. Miedema, *Adv. Phys.*, 1974, **1**, 23.
7 C. Bellitto and P. Day, *J. Mater. Chem.*, 1992, **2**, 265.
8 C. J. Nuttall and P. Day, *Chem. Mater.*, 1998, **10**, 3050.
9 C. J. Nuttall and P. Day, *J. Soid. State Chem.*, 1999, **147**, 3.
10 R. L. Carlin, *Magnetochemistry*, Springer, Berlin, 1986; C. J. O'Connor, *Prog. Inorg. Chem.*, 1982, **29**, 203.
11 L. O. Atovmyan, G. V. Shilov, R. N. Lyubovskaya, E. I. Zhilyaeva, N. S. Ovanesyan, S. I. Pirumova, I. G. Gusakovskaya and Y. G. Morozov, *JETP Lett. Engl. Transl.*, 1993, **58**, 766.
12 G. V. Shilov, N. S. Ovanesyan, N. A. Sanina, A. A. Pyalling and L. O. Atovmyan, *Russ. J. Coord. Chem.*, 1998, **24**, 802.
13 R. B. von Dreele, *General Structure Analysis System*, University of California, 1995.
14 S. Decurtins, H. W. Schmalle, H. R. Oswald, A. Linden, J. Ensling, P. Gütlich and A. Hauser, *Inorg. Chim. Acta*, 1994, **216**, 65.
15 L. J. de Jongh and A. R. Miedema, *Experiments on Simple Magnetic Model Systems*, Taylor & Francis, London, 1974.
16 F. Levy, in *Magnetic Properties of Layered Transition Metal Compounds*, ed. L. J. de Jongh, Kluwer, Dordrecht, 1990, ch. 9.
17 N. S. Ovanesyan, G. V. Shilov, N. A. Sanina, A. A. Pyalling, L. O. Atovmyan and L. Bottyan, *Mol. Cryst. Liq. Cryst.*, 1999, **334**, 803.
18 C. J. Nuttall and P. Day, *Inorg. Chem.*, 1998, **37**, 3885.